Monitoring lysosomal fusion in electrofused hybridoma cells

Mateja Gabrijel [a,b], Marko Kreft [a,b], Robert Zorec [a,b,*]

[a] Celica Biomedical Center, Proletarska cesta 4, 1000 Ljubljana, Slovenia
[b] Laboratory of Neuroendocrinology, Molecular Cell Physiology, Institute of Pathophysiology, Faculty of Medicine, University of Ljubljana, 1000 Ljubljana, Slovenia

Abstract

Dendritic and tumor cells are fused to produce hybridoma cells, which are considered to be used as cellular vaccines to treat cancer. Previous strategies for hybridoma cell production were based on the quantification of the electrofusion yield by labeling the cytoplasm of both parental cell types. However, a better physiological strategy would be to label subcellular structures related directly to the antigen presentation process. Therefore, we here electrofused the same amount of CHO cells stained with red and green fluorescent dextrans and have monitored the yield of hybridoma cell formation by measuring the fusion of red and green late endocytic organelles that are involved in antigen presentation. By using confocal microscopy, the level of fused, fluorescently labelled late endocytic compartments in a single hybridoma cell was determined. The results demonstrate that organellar fusion occurs in hybridomas, which is time- and temperature-dependent. This approach therefore provides a new method for the hybridoma cell vaccine evaluation, which is based on the intracellular physiological mechanism of antigen presentation.
© 2007 Elsevier B.V. All rights reserved.

Keywords: Lysosomal fusion; Quantitative 3D colocalization; Confocal microscopy; Hybridoma cells; Cancer

1. Introduction

Hybridomas between dendritic (DCs) and tumor cells (TCs) represent a cellular vaccine currently considered to be useful for treating cancer. A key step in their production is the determination of fusion yield, which is usually assessed by labeling the cytoplasm of both parental cell types. In this study the aim was to monitor the yield of hybridoma cell formation by measuring the fusion of late endocytic organelles, such as lysosomes.

These are dynamic organelles that obtain membrane and vacuolar contents from endocytosis and *de novo* synthesized enzymes from the Golgi apparatus through the late endosome via vesicle fusion events. It is now well established that lysosomes undergo extensive rounds of self- or homotypic fusion. One reasonable explanation for lysosomal fusion events is the redistribution of substrates for degradation among the population of late endocytic organelles [1].

Fusion of late endocytic organelles also takes place in the antigen presenting process in DCs, which are the major antigen presenting cells (APCs) that constitutively produce molecules of major histocompatibility complex (MHC) class II. These molecules are synthesized in the endoplasmic reticulum of APCs and are transported to late endocytic organelles (often referred to as MHC class II compartments) [2]. The contact between MHC class II molecules and processed peptides is ensured by the fusion of endolysosomes bearing internalized and processed proteins and late endocytic organelles that contain MHC class II molecules [3].

An example of fusion of late endocytic organelles is provided by studies in which cells of the same type are fused to form a heterokaryon. Late endocytic organelles from each partner (which can be identified through either content markers or species-specific lysosomal membrane proteins; e.g., Lamp-1,2) within the heterokaryons show complete intermixing of contents and membrane [4–6]. Interestingly, fusion of these organelles was also detected between different cell types [4]. If antigens from TCs are to be presented by the hybridomas of DCs, fusion events between late endocytic organelles can also be anticipated in hybridoma cells. Specifically, when the MHC

* Corresponding author. Laboratory of Neuroendocrinology, Molecular Cell Physiology, Institute of Pathophysiology, University of Ljubljana, Faculty of Medicine, Zaloska 4, SI-1000, Slovenia. Tel.: +386 1 543 7020.
E-mail address: robert.zorec@mf.uni-lj.si (R. Zorec).

class II–peptide complexes are formed between MHC class II molecules originating from late endocytic organelles of DCs and antigens from late endocytic organelles of TCs [7,8], one would expect that lysosomes from the two cell types get fused. However, this process has not yet been studied.

The aim of the present work was to quantify the extent of hybridoma cells by monitoring the fusion between late endocytic organelles by exposing cells to electrofusion. Fusion of late endocytic organelles was studied in hybridomas consisting of two or more CHO cells stained with red and green fluorescent dextrans, respectively. The level of fused organelles (appearing yellow) in a single hybridoma cell was determined by quantification of the degree of pixel colocalization relative to all red and green pixels in the confocal image [9] and by determining the correlation coefficient for the fluorescence intensities of both confocal channels. The results show that the average number of late endocytic organelles in a CHO cell is 127 ± 22 ($n=21$), consistent with previous reports [10] and that fusion of these organelles is an extensive process in electrofused hybridoma cells. The average rate of fused late endocytic organelles is statistically different between samples incubated at 22 or 37 °C. Moreover, the yields increased as a function of postfusion incubation time as well.

These results therefore show a novel approach for the evaluation of the preparation of whole cell hybridoma vaccines, which is based on the intracellular process of antigen presentation, involving fusion of late endocytic organelles.

2. Materials and methods

2.1. Cell culture

CHO-K1 (Chinese hamster ovary cells; ATCC CRL-1721) were cultured in 25-cm^2 plastic tissue culture flasks at 37 °C, 5% CO$_2$ in Ham's F12-K medium (F12; Sigma, St. Louis, MO), supplemented with 10% fetal bovine serum (FBS, Sigma, St. Louis, MO), 2 mM L-glutamine, 1 U/ml penicillin and 1 µg/ml streptomycin. After the electrofusion, samples were incubated in standard saline solution consisting of 10 mM HEPES/NaOH (pH 7.2), 10 mM D-glucose, 130 mM NaCl, 8 mM CaCl$_2$, 1 mM MgCl$_2$, and 5 mM KCl. All chemicals were obtained from Sigma-Aldrich Inc. (St. Louis, MO).

2.2. Labeling of late endocytic organelles

Cells were incubated with 0.5 mg/ml Alexa Fluor® 546 or 0.5 mg/ml Alexa Fluor® 488 dextrans (10,000 MW; Molecular Probes, OR) for 13 h at 37 °C. The dextran uptake was stopped by rinsing the cultures three times with culture medium at 37 °C. In order to clear marker from early endosomal compartments, cultures were incubated for an additional 3 h at 37 °C in marker-free medium.

2.3. Cell transfection

We used the FuGene transfecting reagent (Roche Applied Science, Indianapolis, IN) according to the manufacturer's instructions to introduce DNA construct Lamp1-EGFP into the cells 24 h following the plating of CHO cells onto glass coverslips. Transfection was performed in essentially the same medium as the culture medium, but without FBS and antibiotics. At the end of transfection, 3% UltroserG (Life Technologies) was added.

2.4. Electrofusion

Stained cells were harvested by treatment with 4% trypsin. Equal proportions of green and red fluorescing cells were washed three times in electrofusion buffer (slightly conductive: 120 µS/cm±10%, at 23 °C, 0.1 mM calcium acetate, 0.1 mM magnesium acetate, 1 mg/ml BSA, pH 7.2±0.2; iso-osmolar 285.0±10

mosmol/kg) ("Isoosmolar electrofusion buffer"; Eppendorf, Hamburg, Germany). We used an Eppendorf Multiporator®, the helix fusion chamber. We also used a custom-made planar fusion chamber, holding up to 5 ml of cell suspension, with a transparent bottom for observation of the ongoing fusion procedure under the microscope in real time. Close contacts between cells were induced by dielectrophoresis for 30 s in the field of 350 V/cm and 2 MHz. The fusion was performed by applying a high voltage pulse (1100 V/cm) for 30 µs and then the cells were exposed to a post alignment field of 350 V/cm, 2 MHz for 30 s. After electrofusion the chamber was opened and the content was rinsed into a container with 1 ml of standard saline solution in which control and electrofused samples were also incubated. The control cells were treated in the same way, except that exposure to the electric field was omitted.

2.5. Confocal microscopy

z-stacks were acquired for each hybridoma cell detected by using a Zeiss LSM 510 confocal microscope with a Plan-Apochromat DIC objective (63×, NA=1.4). Alexa Fluor® 488 dextran was excited by an argon laser at 488 nm and Alexa Fluor® 546 dextran by a He/Ne laser at 543 nm. BP 505–530 nm and LP 560 nm emission filters were used to separate the red and green fluorescence. The sequential collection mode of image acquisition was used to prevent channel cross talk.

2.6. Determination of the number of late endocytic organelles per cell

Confocal microscopy was used to generate z-stacks of 21 randomly selected non-electrofused dextran labeled cells. The average number of late endocytic organelles per cell was obtained by taking into account the average diameter of late endocytic organelles and the average thickness of optical slices. The diameters of 40 randomly selected late endocytic organelles were measured manually using LSM Carl Zeiss software. According to the pinhole diameter and NA, the optical slice thickness was set to 0.5 µm. Organelles were quantified using the custom ParticleCO software [11] under the assumption that each organelle can appear in three adjacent optical slices.

2.7. Determination of the extent of hybridoma cells

The percentage of hybridomas was estimated by counting cells that contained at lest 30 red and 30 green or at least 30 yellow late endocytic organelles and usually at least two nuclei. At least 300 randomly selected cells were considered in the analysis of a sample. The image of the cells was scanned systematically from the top left corner by an evaluation square (1/9th of the area of the image) in which all the cells were counted starting from the row on the left, counting to the right, line after line. When the counting in the evaluation square was completed, the field was moved one step towards the right and the procedure was repeated until the whole image was analyzed. The percentage of hybridoma cells was expressed as the percentage of cells containing at lest 30 red and 30 green or at least 30 yellow organelles and usually at least two nuclei, in relation to all the cells counted.

2.8. Determination of the extent of fused late endocytic organelles in hybridoma cells

The average percentage of colocalized pixels in each optical slice was assessed by automated evaluation of colocalized pixels relative to all red and green fluorescent pixels [9]. The contrast of all images was uniformly set by linearly reassigning the value of the pixel intensities to use the full 8 bit range (0–255). We determined the threshold value, which separated the background intensity levels from the signal of single red and green pixels. The value 51 a.u. of 255 intensity levels, which corresponds to 20% of the maximum intensity level, was selected. In addition to thresholding, Pearson's r correlation coefficient was calculated for fluorescence intensities of both confocal channels.

3. Results

Previous strategies for hybridoma cell production were based on quantification of the electrofusion yield by labeling the cytoplasm of both parental cell types. However, a better

physiological strategy would be to label subcellular structures related directly to the antigen presentation process. Therefore, here we have monitored the yield of hybridoma cell formation by measuring the fusion of late endocytic organelles involved in antigen presentation [6].

3.1. Fluorescent dextran labels late endocytic organelles in CHO cells

In order to observe fusion of late endocytic organelles, we labeled the same number of CHO cells with either 0.5 mg/ml red fluorescent Alexa Fluor® 546 or 0.5 mg/ml green fluorescent Alexa Fluor® 488 dextran as described in Materials and methods [5]. Fig. 1a represents a CHO cell with 105 punctate subcellular structures labeled by fluorescent dextran, likely representing late endocytic organelles.

To verify that the dextran loaded organelles represent late endocytic organelles such as lysosomes, CHO cells were incubated in red fluorescent dextran (Fig. 1b) and transfected
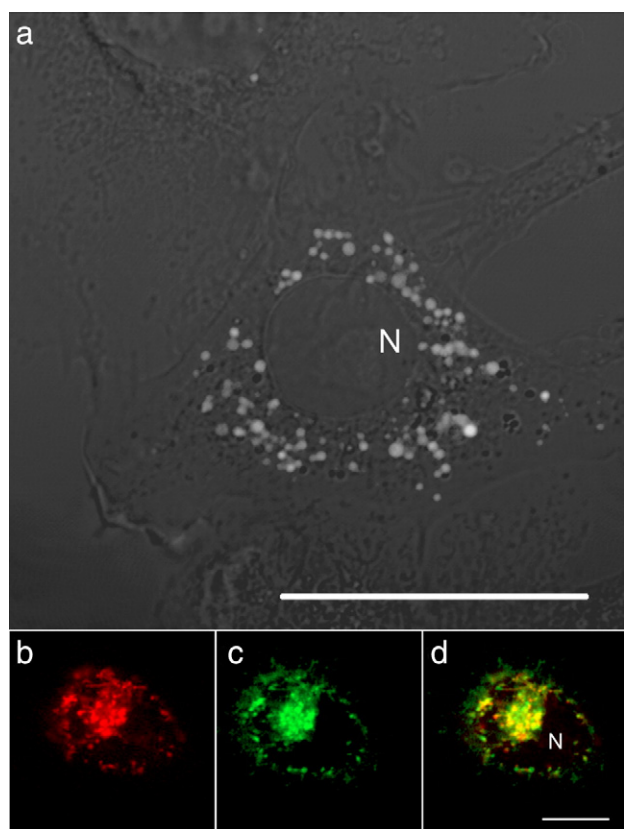

Fig. 1. Fluorescent dextran labels granular compartments in CHO cells. (a) The CHO cells were loaded with either Alexa Fluor® 546 or Alexa Fluor® 488 dextran. The micrograph represents a CHO cell with granular subcellular compartments stained by dextran fluorescence, representing lysosomes. Note the relatively large nucleus in the middle of the cell (N). The number of fluorescence puncta in this optical slice was 105. Scale bar: 30 μm. (b) Dextran fluorescence is shown in red. (c) The expression of Lamp1-EGFP is seen as green fluorescence. (d) Areas of colocalization appear in yellow in the composite image. The percentage of colocalized pixels in this image was 91%. Scale bar: 15 μm.
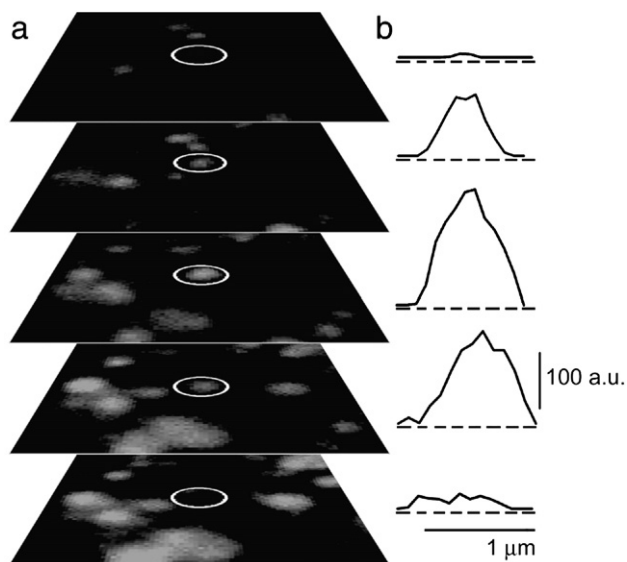
with the Lamp 1-EGFP fusion construct, which codes for the lysosomal associated membrane protein (Lamp1), a 120-kDa highly glycosylated membrane protein enriched in the membrane of lysosomes [12] and the green fluorescent protein EGFP. The expression of Lamp 1-EGFP resulted in green fluorescence (Fig. 1c), which appears colocalized with the red dextran label. Areas of colocalization appear in yellow in the composite image (Fig. 1d). The degree of colocalization was determined by estimating the level of colocalized red and green pixels relative to all red fluorescent pixels in each optical slice of the acquired z-stack of images (described in Materials and methods). The results show that the average percentage of colocalized pixels in the cells analyzed was $90 \pm 2\%$ ($n = 10$).

3.2. Identification of hybridoma cells

To obtain hybridoma cells we fused the same number of red and green dextran loaded cells in a high voltage field. Electrofused and control samples, for which the exposure to the high voltage field was omitted, were then incubated in standard saline solution at 22 or at 37 °C for various time intervals (6, 12, 20 h). Afterwards samples were fixed and analyzed for the presence of hybridomas by confocal microscopy. A hybridoma cell was considered to contain at least a minimal number of red, green and yellow late endocytic organelles. Therefore we first counted the average number of late endocytic organelles per cell. We acquired confocal z-stacks of images in 21 randomly selected dextran loaded, non-electrofused cells. The number of labeled organelles per cell was counted considering the possibility that each organelle can appear in more than one optical slice. Given the average diameter of late endocytic organelle to be 1.11 μm and the optical section thickness of 0.5 μm, an organelle could potentially span over three optical lines. However, the appearance of a late endocytic compartment in two or three optical planes was considered to represent only one organelle (Fig. 2). The average number of late endocytic organelles per cell was 127 ± 22 ($n = 21$), whereas the minimum number of late endocytic organelles per cell was 30. Therefore we set the threshold in a cell to 30 organelles, in order to carry out the analysis of hybridoma cell yields, expressed as a percentage of all cells examined. For each hybridoma cell detected, which also typically included at least two nuclei, in electrofused and control samples, we acquired z-stacks and counted late endocytic organelles [11].

3.3. Time- and temperature-dependence of hybridoma cell fusion rates

The confocal image in Fig. 3a represents an image of cells exposed to electrofusion. In two populations of cells, late endocytic compartments were labeled by red and green fluorescent dextrans, respectively. The frame in Fig. 3a indicates a hybridoma cell that is enlarged in Fig. 3b. The yellow color in the image represents fused (red and green) organelles.

The results in Fig. 3c indicate that the temperature did not significantly affect the average percentage of fused hybridoma

Fig. 2. Determination of the number of late endocytic organelles in a cell. To estimate the number of late endocytic organelles per cell we acquired *z*-stacks of dextran loaded CHO cells. The step size (*z*-axes) of the optical slices was 0.5 μm, according to the Nyquist criterion. Labeled late endocytic organelles were counted considering the possibility that an organelle can appear in more than one optical slice, which is due to the lysosome size and the step size. (a) A series of vertical optical slices. The step size (*z*-axes) of the optical slices was 0.5 μm. The circles indicate a selected organelle through which a line intensity profile was drawn in (b). The series of graphs represent line intensity profiles indicating that an image of a late endocytic organelle may span over three optical slices.

sion into the *z*-axis (Fig. 4). The estimated probability for false detection was extremely small (1×10^{-5}), since the probability of observing a late endocytic organelle in any *x,y* cell plane was around 3×10^{-3}, as determined by measuring the area of a cell, which was over 30,000 pixels, and that of a late endocytic organelle, which was less than 100 pixels. The extent of apparently fused late endocytic organelles, containing red and green fluorescent dyes, was determined by calculating the number of red, green and colocalized pixels for each optical slice in the acquired z-stack. Colocalized pixels were then expressed as a percentage of all red and green pixels in each hybridoma cell. The percentages of colocalized pixels determined for each hybridoma cell were then averaged to obtain the general percentage of fused late endocytic organelles at 22 or 37 °C at a specific time of
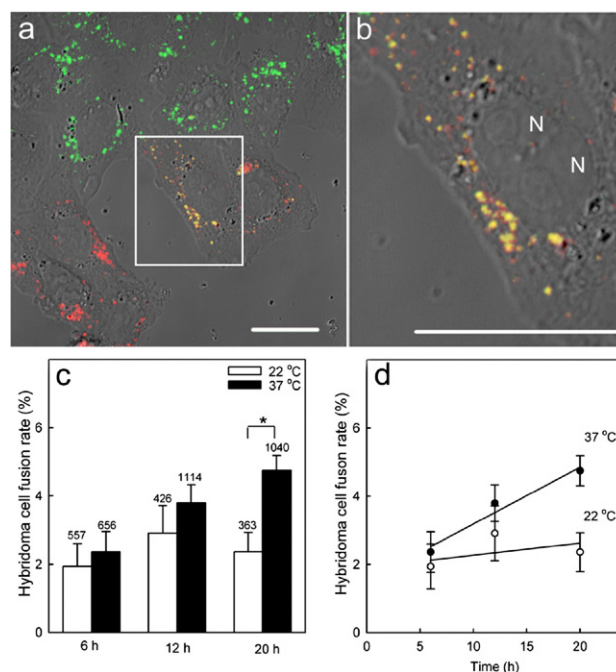

Fig. 3. The appearance of hybridoma cells in the electrofused samples. (a) A representative confocal image (overlay of a DIC and red and green fluorescent channels) of cells exposed to electrofusion. Cells were labeled by red and green dextrans and incubated for 20 h at 37 °C. The frame highlights a hybridoma cell, determined as a cell that contains at least 30 red and 30 green or 30 yellow (red and green) fluorescent late endocytic organelles and two nuclei, marked by N. (b) An enlargement of the box in (a). Yellow represents fused (red and green) organelles in the hybridoma cell. In this image the average colocalization between red and green pixels was 75%. Scale bar: 20 μm. (c) The average percentage of counted electrofused hybridoma cells is not significantly affected by the length of incubation (6 and 12 h), if the temperature is 22 or 37 °C. A 6-h incubation yielded an average fusion rate of 1.9±0.7% (*n*=557) at 22 °C and 2.4±0.6% (*n*=656; *P*=0.636; Student's *t*-test) at 37 °C. A 12-h incubation yielded an average fusion rate of 2.9±0.8% (*n*=426) at 22 °C and 3.8±0.5% (*n*=1114; *P*=0.349; Student's *t*-test) at 37 °C. However, in samples incubated for 20 h, the hybridoma cell fusion rates detected were statistically different (fusion rate at 22 °C: 2.4±0.6%, *n*=363; fusion rate at 37 °C: 4.7±0.4%, *n*=1040; *P*=0.002; Student's *t*-test). (d)The regression lines show the correlation between the percentage of hybridoma cell fusion as a function of time at 22 and 37 °C. At 22 °C the line is in the format: hybridoma cell fusion rate[%]=(0.0±0.1)×time[h]+(1.9±0.9); *n*=54)) and at 37 °C the line is in the format: hybridoma cell fusion rate[%]=(0.2±0.1)×time[h]+(1.5±0.7); *n*=63.

cells, if samples were incubated for 6 h (Fig. 3c) or 12 h (Fig. 3c). However, incubation for 20 h at 37 °C resulted in a statistically increased fusion rate of hybridoma cells (Fig. 3c). The regression analysis shown in Fig. 3d is consistent with these results. At 37 °C the regression line has the format: hybridoma cell fusion rate[%]=(0.2±0.1)×time[h]+(1.5±0.7); the slope is statistically different from zero (*P*=0.002), whereas the intercept is not. The correlation coefficient of the regression analysis is *R*=0.38 (significantly different from zero, *P*=0.002, *n*= 63). In contrast, the time-dependence of the rate of hybridoma fusion was not significantly different when samples were incubated at 22 °C. The regression line has the format: hybridoma cell fusion rate [%]=(0.0±0.1)×time[h]+(1.9±0.9); *R*=0.08, *P*=0.587, *n*=54, (Fig. 3d). The slope and the intercept of the line are not significantly different from zero. Therefore, we concluded that the formation of hybridoma cells is time dependent at 37 °C.

The fusion rate in control non-electrofused samples was 0% (*n*=998) when samples were incubated at 22 or at 37 °C.

3.4. The percentage of fused late endocytic organelles in hybridoma cells

Next we investigated the extent of apparent fusion of late endocytic organelles in a hybridoma cell. An organelle was considered fused if a double labeled red and green lysosome, appearing yellow, was detected among the red and green ones. To confirm that the yellow organelles were not due to overlay (overlapping) of red and green organelles, *z*-stacks were recorded and images carefully analyzed by tracing object exten-
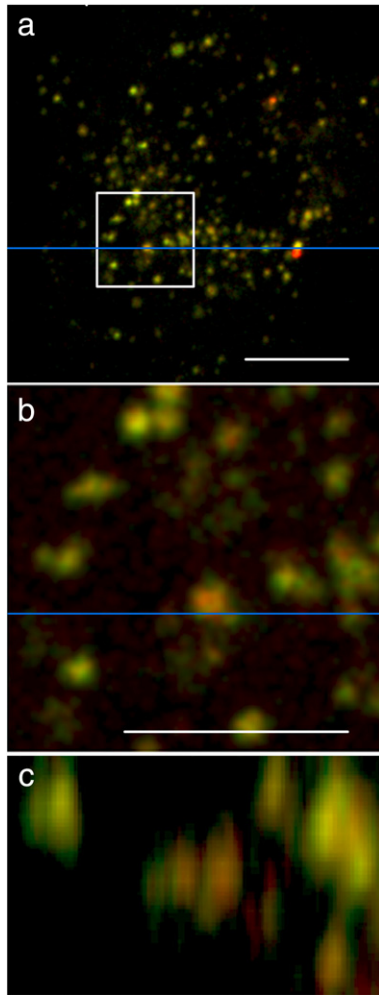
Fig. 4. The appearance of yellow late endocytic organelles is not a consequence of the vertical apposition of red and green organelles. Following electrofusion, we measured the level of fused organelles in each hybridoma cell detected. To confirm that yellow organelles were not due to close vertical apposition of red and green organelles, we acquired z-stacks. (a) The confocal image represents a hybridoma cell that contains labeled compartments in the *x*,*y* plane. The frame indicates a cluster of yellow organelles, which are enlarged in the micrograph (b) in the *x*,*y* plane. (c) A vertical section, taken as indicated by the blue line, drawn in (a) and (b), showing a fused red and green late endocytic compartment appearing yellow. Note that the yellow pixels extend into the *x*,*z* plane, indicating that groups of pixels appearing yellow in the *x*,*y* plane are not due to vertical apposition of red and green pixels. Scale bar: 10 μm.

tionally, the relationship between red and green channel intensities revealed a strong correlation coefficient (Fig. 5f) in the hybridoma cells incubated at 37 °C ($R=0.84$), whereas a weak correlation coefficient was found at 22 °C ($R=0.35$) (Fig. 5c).

Fig. 5g shows the average rate of fusion of late endocytic organelles, determined by colocalization analysis, to be statistically different in samples incubated both at 22 and 37 °C. Moreover, it is clear from Fig. 5h that the yields of fusion of late endocytic organelles were time-dependent. However, the time-dependent increase in apparent fusion of organelles was higher at a higher temperature of incubation. The results presented in Fig. 5h show a significant correlation between the average percentage of fused late endocytic organelles in hybridoma cells and the time of incubation of the electrofused samples at 22 °C ($R=0.39$, $P=0.015$, $n=41$) or 37 °C ($R=0.49$, $P<<0.001$, $n=105$). Both lines were obtained with linear regression. The line representing apparent fusion at 22 °C is in the format: fusion rate of late endocytic organelles[%]$=(0.9\pm0.4)\times$time[h]$+(-4.1\pm5.5)$ (the intercept is not statistically different from zero, whereas the slope is ($P=0.015$)), compared to the line representing samples incubated at 37 °C: fusion rate of late endocytic organelles[%]$=(1.7\pm0.3)\times$time[h]$+(9.4\pm4.7)$. The intercept of the line is not statistically different from zero, whereas the slope is ($P<<0.001$).

In addition to the method based on thresholding, the level of colocalized pixels in each optical slice of a hybridoma cell was evaluated by determining the correlation coefficient for the fluorescence intensities of both confocal channels. At any time point, the estimated values of Pearson's correlation coefficients, as shown in Fig. 5i, were significantly higher at 37 °C than at 22 °C. Moreover, correlation coefficients increase like the estimated percentages of fusion rates of late endocytic organelles along with the incubation time (Fig. 5i). The time- and temperature-dependent colocalization of red and green pixels, representing subcellular organelles arising from distinct cells, evaluated in two different ways, is consistent with the fusion of late endocytic organelles that are involved in the antigen presentation pathway.

4. Discussion

Theoretically, DC-TC hybridomas possess potent antigen presenting capacities of DCs and are therefore capable of processing and presenting known and unknown tumor antigenic peptides within the context of their MHC class I and class II molecules, as well as costimulatory ligands and receptors, necessary for evoking primary CD4+ and CD8+ T cell responses [13].

An important aspect of any electrofusion-based application is the ability to assess the yield of DC-TC hybridomas since the concentration of these cells is thought to decisively mediate the extent of the immune response [14]. Therefore, the adequate approach for detection and quantification of the electrofusion products it is of key importance. In the recent past, researchers have relied primarily on flow cytometry [15] or on confocal microscopy, which is a more sensitive and objective method [16]. The labeling of the cytoplasm of both parental cell types

incubation. However, the quantification of colocalized pixels in the hybridoma cell provides only the minimum estimation for the fusion rate of late endocytic organelles.

Optical slices shown in Fig. 5a and d represent hybridoma cells detected in electrofused samples incubated for 20 h at 22 °C (Fig. 5a) and 37 °C (Fig. 5d), respectively. Analysis of the extent of fusion of late endocytic organelles by the colocalization of pixels is displayed in white as the colocalization mask (Fig. 5b and e). Note that a larger white (overlapping) area was determined in hybridoma cells incubated at 37 °C (46%, Fig. 5e) in comparison with that obtained at 22 °C (14%, Fig. 5b). Addi-
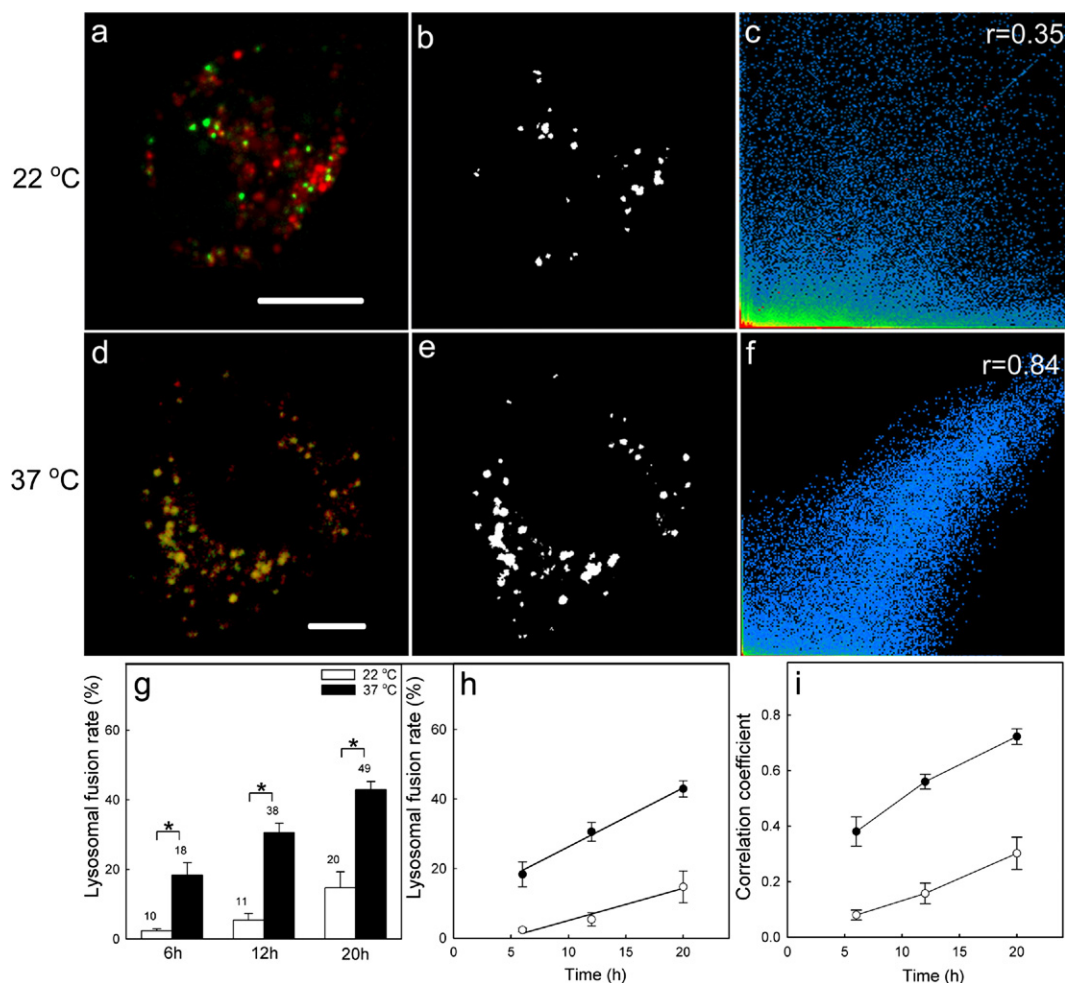
Fig. 5. The extent of fusion of late endocytic organelles in hybridoma cells. Optical sections of hybridoma cells detected in electrofused samples incubated for 20 h at 22 °C (a) and at 37 °C (B) that were analyzed for the presence of colocalized pixels. Micrographs (b) and (e) represent the colocalization mask of each optical section. Note the higher degree of overlap in the colocalization mask of hybridoma cells detected at 37 °C in comparison to hybridoma cells detected at 22 °C. The scatter plots in (c) and (f) display the intensity range of red, green and colocalized pixels of the corresponding optical section, as well as the degree of correlation between both channels. Note the lower degree of correlation ($R=0.35$) in the scatter plot (c) in comparison to the scatter plot in the micrograph (f) ($R=0.84$). Graph (g) illustrates the estimated average percentage of colocalized pixels using the method based on thresholding. The minimal estimation of the fusion rate of fused lysosomes is statistically different in samples incubated at 22 or 37 °C for 6 h (average fusion rate at 22 °C: $2.4\pm0.5\%$, $n=10$; at 37 °C: $18.4\pm3.6\%$, $n=18$; $P=0.002$; Student's t-test), 12 h (average fusion rate at 22 °C: $5.4\pm1.9\%$, $n=11$; at 37 °C: $30.6\pm2.7\%$, $n=38$; $P\ll0.001$; Student's t-test) or 20 h (average fusion rate at 22 °C: $14.8\pm4.6\%$, $n=20$; at 37 °C: $43.0\pm2.3\%$, $n=49$; $P\ll0.001$; Student's t-test). The results in graph (h) show significant correlation between the average percentage of fused late endocytic organelles in hybridoma cells and the time of the incubation of the electrofused samples at 22 °C or 37 °C. Both lines were obtained with linear regression. The line that represents apparent fusion of late endocytic organelles in samples incubated at 22 °C is in the format: fusion rate of late endocytic organelles[%]=$(0.9\pm0.4)\times$time[h]+(-4.1 ± 5.5), whereas the line that represents the apparent lysosomal fusion in samples incubated at 37 °C is in the format: fusion rate of late endocytic organelles[%]=$(1.7\pm0.3)\times$time[h]+(9.4 ± 4.7). Graph (i) shows the values of Pearson's r correlation coefficients estimated for hybridoma cells detected at 22 or 37 °C for 6 h (at 22 °C: 0.1 ± 0.0, $n=10$; at 37 °C: 0.4 ± 0.1, $n=18$; $P\ll0.001$; Student's t-test), 12 h (at 22 °C: 0.2 ± 0.0, $n=11$; at 37 °C: 0.6 ± 0.0, $n=38$; $P\ll0.001$; Student's t-test) or 20 h (at 22 °C: 0.3 ± 0.1, $n=20$; at 37 °C: 0.7 ± 0.0, $n=49$; $P\ll0.001$; Student's t-test). Scale bar: 10 μm.

was typically employed in both techniques. However, a better physiological strategy would have been more appropriate to characterize hybridoma cells, for example by labeling the subcellular structures that are involved directly in the antigen presentation pathway.

In the present study we first labeled the late endocytic organelles of CHO-K1 cells (Fig. 1a) and then fused them in order to monitor putative fusion of late endocytic organelles. Moreover, this process was considered as a method to determine the yield of hybridoma cells. Late endocytic organelles were identified through Lamp1, a species-specific lysosomal mem-

brane protein (Fig. 1c). As shown in Fig. 1d, subcellular structures loaded with red fluorescent dextran colocalized by 90% with the green fluorescence tagged lysosomal marker, Lamp1-EGFP. From these results we can conclude that dextran is localized to a large extent in late endocytic structures in the studied cells. Electrofused and control samples were incubated for 6, 12 or 20 h at 22 or 37 °C. Cells were defined as hybridomas when they contained at least a minimum number of red, green, or yellow (red and green) fluorescent organelles (Fig. 3). The number of late endocytic organelles in a cell was evaluated by generating z-stacks of randomly selected non-

electrofused dextran labeled cells, subjected to 3D counting, assuming that each organelle may appear in three optical slices (Fig. 2). The average number of late endocytic organelles per cell was 127 ± 22 ($n=21$), whereas the minimum number per cell was 30, consistent with previous reports [10]. The average percentage of hybridoma cells detected in electrofused samples at 22 °C was not significantly affected by the incubation time (Figs. 3c and d). This was expected, since endocytosis and vesicular trafficking of the membrane are virtually stopped at this temperature [17,18]. However, the change of temperature to 37 °C resulted in a detectable increase in the percentage of hybridoma cells as a function of incubation time. The maximum hybridoma fusion rate of $5\pm0\%$ ($n=1040$, $P=0.002$; Student's t-test) was observed when samples were incubated for 20 h at 37 °C. In the absence of the electric field, the extent of the hybridoma cells was 0% ($n=998$), regardless of whether the samples of CHO cells were incubated at 22 or 37 °C.

To quantify the extent of the fusion product, we determined the level of colocalized red and green late endocytic organelles in each hybridoma cell detected. To confirm that the yellow compartments were not due to close vertical apposition of red and green organelles, optical slices of z-stacks were examined by tracing the object extension into the z-axis (Fig. 4). The level of fused late endocytic organelles was then estimated by calculating the number of colocalized pixels, relative to all red and green late endocytic organelles, for each optical slice. Pixels were considered as colocalized when the intensity of both the red and green channels exceeded the threshold value of 51 a.u. The uniform threshold level was determined by the analysis of non-electrofused control samples, where the red and green fluorescent dextrans were not colocalized. Since vesicular trafficking is sensitive to lower temperatures, the actual overlap between red and green dextran fluorescence in electrofused hybridoma cells at any time point is expected to be greater at 37 °C than at 22 °C [17]. Indeed, hybridoma cells showed a reduced coincidence of fluorescent dextrans when samples were incubated at 22 °C in comparison to those kept at 37 °C at any experimental time point of incubation (Fig. 5). Moreover, the apparent fusion of late endocytic organelles increased as a function of incubation time. The highest level of colocalization of red and green late endocytic organelles per cell, $43\pm2\%$ ($n=49$, $P\ll0.001$; Student's t-test) was observed when samples were incubated for 20 h at 37 °C.

Because the fluorescent signal in the optical slices was not distributed in an all or nothing manner, we also quantified the colocalization, in addition to the thresholding approach, by calculating the correlation coefficient for the fluorescence intensities of both the red and green channels. The correlation coefficients indicated an increasing degree of colocalization in hybridomas incubated at 22 or 37 °C, as a function of incubation time (Fig. 5i). Coefficients calculated for hybridomas that were detected at 22 °C were lower in comparison to those defined at 37 °C, at any time point of incubation. All of these comparisons were found to be statistically significant ($P\ll0.001$; Student's t-test). The highest degree of colocalization as defined by correlation coefficients in hybridomas incubated for 20 h at 37 °C (0.7 ± 0.0, $n=49$). These results are consistent with the colocalization values estimated by the thresholding method.

We conclude that the approach of monitoring the fusion of late endocytic organelles is suitable for determining hybridoma cell yields, which are significantly higher when the electrofused samples are incubated at 37 °C than at 22 °C. It is interesting to note that previously determined parameters for obtaining hybridomas were limited to an incubation of 2 h following electrofusion [19]. However, the results in this study show that a higher fusion rate is achieved by a longer incubation after exposure to electrofusion. While the actual higher immunogenic potential of DC-TC hybridomas with fully fused late endocytic organelles awaits further studies, it is likely that monitoring the yield of hybridomas by measuring the fusion of late endocytic organelles represents a new paradigm, based on the physiologically related antigen presentation [20].

Acknowledgments

References

[1] D.M. Ward, J.D. Leslie, J. Kaplan, Homotypic lysosome fusion in macrophages: analysis using in vitro assay, J. Cell Biol. 139 (1997) 665–673.

[2] R.F. Wang, The role of MHC class II-restricted tumor antigens and CD4+ T cells in antitumor immunity, Trends Immunol. 22 (2001) 422–423.

[3] C. Watts, Capture and processing of exogenous antigens for presentation on MHC molecules, Annu. Rev. Immunol. 15 (1997) 821–850.

[4] Y. Deng, B. Storrie, Animal cell lysosomes rapidly exchange membrane proteins, Proc. Natl. Acad. Sci. U. S. A. 85 (1988) 3860–3864.

[5] Y. Deng, G. Griffiths, B. Storrie, Comparative behavior of lysosomes and the pre-lysosome compartment (PLC) in vivo cell fusion experiments, J. Cell Sci. 99 (1991) 571–582.

[6] A.L. Ferris, J.C. Brown, R.D. Park, B. Storrie, Chinese hamster ovary cell lysosomes rapidly exchange contents, J. Cell Biol. 105 (1987) 2703–2712.

[7] Y. Akasaki, T. Kikuchi, S. Homma, T. Abe, D. Kofe, T. Ohno, Antitumor effect of immunizations with fusions of dendritic and glioma cells in a mouse brain tumor model, J. Immunother. 24 (2001) 106–113.

[8] M. Lindner, V. Schirrmacher, Tumour cell–dendritic cell fusion for cancer immunotherapy: comparison of therapeutic efficiency of polyethylen-glycol versus electro-fusion protocols, Eur. J. Clin. Investig. 32 (2002) 207–217.

[9] M. Kreft, I. Milisav, M. Potokar, R. Zorec, Automated high through-put colocalization analysis of multichannel confocal images, Comput. Methods Programs Biomed. 74 (2004) 64–67.

[10] L.A. Marshall, M.S. Rhee, L. Hofmann, A. Khodjakov, E. Schneider, Increased lysosomal uptake of methotrexate-polyglutamates in two methotrexate-resistant cell lines with distinct mechanisms of resistance, Biochem. Pharmacol. 71 (2005) 203–213.

[11] M. Kreft, R. Zorec, Particle CO: particle counting software: user's guide. Celica, Ljubljana, Slovenia, 2005. URL: http://lnmcp.mf.uni-lj.si/particleCO_guide.pdf.

[12] C.L. Howe, B.L. Granger, M. Hull, S.A. Green, C.A. Gabel, A. Helenius, I. Mellman, Derived protein sequence, oligosaccharides, and membrane insertion of the 120-kDa lysosomal membrane glycoprotein (Igp120): identification of a highly conserved family of lysosomal membrane glycoproteins, Proc. Natl. Acad. Sci. U. S. A. 85 (1988) 7577–7581.

[13] G. Schuler, R.M. Steinman, Dendritic cells as adjuvants for immune-mediated resistance to tumor, J. Exp. Med. 186 (1997) 1183–1187.

[14] T. Hayashi, H. Tanaka, J. Tanaka, R. Wang, B.J. Averbook, P.A. Cohen, S. Shu, Immunogenicity and therapeutic efficacy of dendritic-tumor hybrid cells generated by electrofusion, Clin. Immunol. 104 (2002) 14–20.

[15] M.J. Jaroszeski, R. Gilbert, R. Heller, Detection and quantitation of cell–cell electrofusion products by flow cytometry, Anal. Biochem. 216 (1994) 271–275.

[16] M. Gabrijel, U. Repnik, M. Kreft, S. Grilc, M. Jeras, R. Zorec, Quantification of cell hybridoma yields with confocal microscopy and flow cytometry, Biochem. Biophys. Res. Commun. 314 (2004) 717–723.

[17] W.A. Dunn, A.L. Hubbard, N.N. Aronson Jr., Low temperature selectively inhibits fusion between pinocytic vesicles and lysosomes during hetero-phagy of 125I-asialofetuin by the perfused rat liver, J. Biol. Chem. 255 (1980) 5971–5978.

[18] P.C. Sullivan, A.L. Ferris, B. Storrie, Effects of temperature, pH elevators, and energy production inhibitors on horseradish peroxidase transport through endocytic vesicles, J. Cell Physiol. 131 (1987) 58–63.

[19] S.E. Strome, S. Voss, R. Wilcox, T.L. Wakefield, K. Tamada, D. Flies, A. Chapoval, J. Lu, J.L. Kasperbauer, D. Padley, R. Vile, P. Gastineau, L. Wettstein, Chen, Strategies for antigen loading of dendritic cells to enhance the antitumor immune response, Cancer Res. 62 (2002) 1884–1889.

[20] M.J. Kleijmeer, M.A. Ossevoort, C.J. van Veen, J.J. van Hellemond, J.J. Neefjes, W.M. Kast, C.J. Melief, H.J. Geuze, MHC class II compartments and the kinetics of antigen presentation in activated mouse spleen dendritic cells, J. Immunol. 154 (1995) 5715–5724.